Details:

Title: Analytical prediction of seismicity rate due to tides and other oscillating stresses

Authors:

Elías Rafn Heimisson (Caltech)
Jean-Philippe Avouac (Caltech)

Contact: eheimiss@caltech.edu

Analytical prediction of seismicity rate due to tides and other oscillating stresses

Elías R. Heimisson[1], and Jean-Philippe Avouac[1]

[1]Division of Geological and Planetary Sciences, California Institute of Technology, Pasadena, CA, USA

Key Points:

- We derive a simple analytical model for seismicity rate based on rate-and-state friction
- The model can be applied to perpetually oscillating stresses on Earth and other solid-surface bodies
- We reevaluate recent work on possible tidally triggered seismicity on Mars

Corresponding author: Elías R. Heimisson, `eheimiss@caltech.edu`

Abstract

Oscillatory stresses are ubiquitous on Earth and other solid-surface bodies. Tides and seasonal signals perpetually stress faults in the crust. Relating seismicity rate to these stresses offers fundamental insight into earthquake triggering. We present a simple model that describes seismicity rate due to perpetual oscillatory stresses. The model applies to large amplitude, non-harmonic, and quasi-periodic stressing histories. However, it is not valid for long periods, which are larger than a characteristic time t_a. We show that the seismicity rate from a short period stressing scales with the stress amplitude, but for long periods, the stressing rate. We suggest that parameter $A\sigma_0$ may be underestimated if stresses are approximated by a single harmonic function. We revisit Manga et al. (2019), which analyzed the potential tidal triggering of Marsquakes. We find that the maximum response of the seismicity on Mars was likely overestimated by over one order of magnitude.

Plain Language Summary

The surface of the Earth, and many other planets and moons, is constantly being stressed in an oscillatory manner, for example, by the gravitational pull of moons, planets, and suns. Further, the weather, climate, oceans, and other factors may also generate oscillatory stresses. The resulting fluctuations in stress may result in an increased or decreased probability of earthquakes with time. Here we derive a simple formula that can help scientists understand how these oscillatory stresses relate to seismic activity. Moreover, we revisit a recent estimate of the maximum sensitivity of Marsquakes to oscillatory stresses and find that it was likely overestimated.

1 Introduction

Faults in the shallow crust are submitted to perpetual, quasi–periodic, oscillatory stress perturbations due to a number of forcing factors. In particular, oceanic or solid earth-tides, seasonal surface loads due to surface hydrology and the cryosphere, and surface temperature changes. The study of the seismicity response to such stress variations can in principle provide insight into fault friction and earthquake nucleation mechanisms (e.g. Beeler & Lockner, 2003; Scholz et al., 2019; Luo & Liu, 2019; Ader et al., 2014) and possibly inform us on the preparatory phase to impending earthquakes (e.g. Chanard et al., 2019; Tanaka, 2012). On Mars and the Moon, such factors might actually be the dominant source of seismicity (Manga et al., 2019; Duennebier & Sutton, 1974; Lognonne, 2005).

Stresses from oscillatory loading are temporally complex but can be computed with reasonable accuracy (e.g. Lu et al., 2018; Johnson et al., 2020), their relationship to changes in seismicity or tremor rate might reveal fundamental insight into earthquake triggering. While tectonic tremors seem strongly correlated to tides both in the roots of strike-slip faults (Thomas et al., 2012, 2009) and subduction zones (Rubinstein et al., 2008; Yabe et al., 2015; Houston, 2015). It has also been observed that slow slip can be modulated by tidal stresses (Hawthorne & Rubin, 2010). Seasonal variation of seismicity driven by surface load variations have been reported in a number of studies (e.g. Bettinelli et al., 2008; Amos et al., 2014; Ueda & Kato, 2019). However, in most places, the seismicity rate depends weakly on tides (Tanaka et al., 2002; Cochran et al., 2004), except at mid-ocean ridges where a particularly strong response has been observed (e.g. Tolstoy et al., 2002). With the emergence of the next generation of machine learning and template matching techniques for generating earthquake catalogs, which may have ten times the sensitivity of traditional methods (e.g. Ross et al., 2019), we will be able to detect and quantify the seismicity response to tidal and seasonal loading. New developments in observational earthquake seismology, as well as the emplacement of a seismometer on Mars, call for a simple model for seismicity rate under tidal loading that can be compared to data, here we provide such a model (equation 15) that can be readily used and has effectively only one free parameter in most applications.

Theoretical studies to date have used the rate-and-state seismicity production model of Dieterich (1994) to develop an approximate theory for oscillatory stresses. Dieterich (2007) recognized that for small amplitude and short duration stress changes, the tidally induced signal could be approximated as the instantaneous response predicted by the Dieterich (1994) theory. Under these assumptions, Dieterich (2007) derived a simple relationship for a harmonic stress perturbation. Ader et al. (2014) provided a more general analytical expression and showed that once some of the assumptions made by Dieterich (2007) no longer hold the response is not simply the instantaneous response; however, the analysis of Ader et al. (2014) was also restricted to a single harmonic perturbation. Because rate-and-state friction is highly non-linear, knowing the response to harmonic perturbations is not sufficient to describe the response to oscillatory stress variations in general. For example, tidal loading can not be explained by a single harmonic perturbation (e.g. Figure 1) and the formalism of Dieterich (2007) and Ader et al. (2014) would not allow estimating the expected seismicity response. We, therefore, present a simple approximate relationship for seismicity rate due to arbitrary long-term oscillatory stressing that is superimposed on the long-term constant stressing rate. The oscillatory stressing can be non-harmonic, quasi-periodic, and include random variations. The approximation is typically valid as long as the average of the oscillatory stress is zero on timescale shorter than a characteristic time t_a. We give a mathematical condition for when the approximation is valid and provide corrections and alternative expressions for end-member cases where the approximation breaks down. As an illustration, we show that our solution predicts a seismicity response to seasonal forcing on Mars that is significantly different from that predicted by Manga et al. (2019) based on the solution of Dieterich (1994).

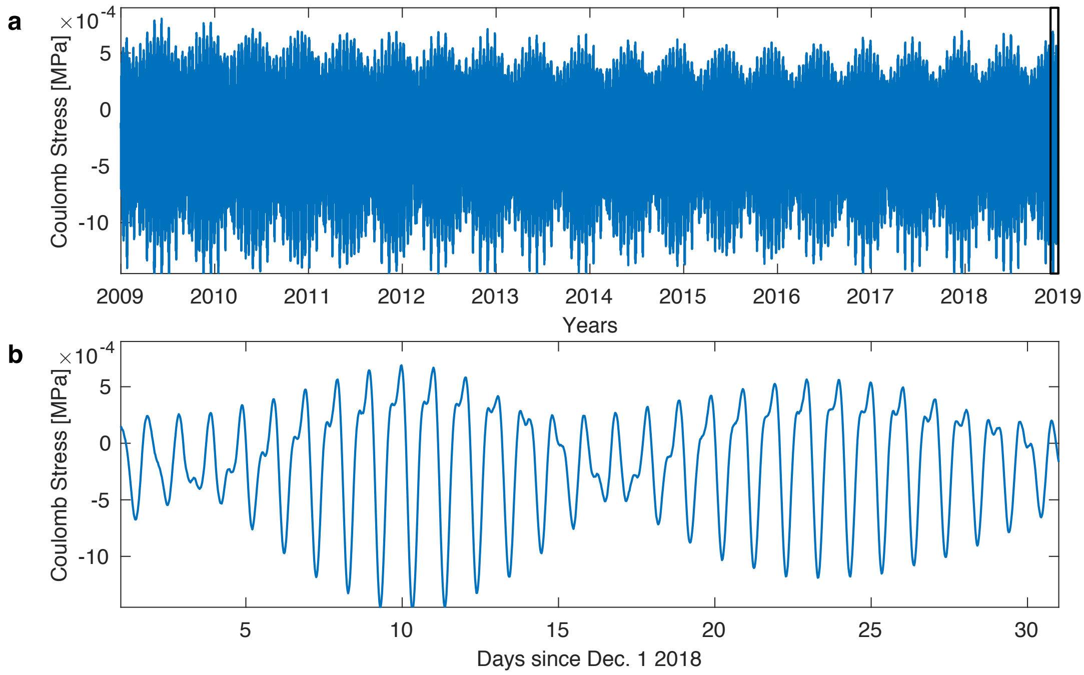

Figure 1. Time-series of Coulomb stress changes due to the solid earth tides.(a) 10 years of Coulomb stress perturbations due to solid earth tides on a shallow right-lateral strike-slip fault striking NW-SE and located at Caltech campus. (b) The stress changes in the black box in (a). In section 3.1 we will compute the theoretical seismicity rate during the period in (b) where the entire time-series in (a) is used to fade out the instantaneous initial response.

2 Theory

Heimisson and Segall (2018) re-derived the Dieterich (1994) theory and showed:

$$R(t) = r\frac{K(t)}{1+\frac{1}{t_a}\int_0^t K(t')dt'}, \tag{1}$$

where $R(t)$ is the seismicity rate produced by a populations of seismic sources with background seismicity rate r. See Heimisson (2019) for a detailed definition of the concept of a population of seismic sources. Further, Heimisson and Segall (2018) showed that if changes in normal stress $\sigma(t)$ are small compared to the initial normal stress σ_0 then K is well approximated as:

$$K(t) \approx \exp\left(\frac{S(t)}{A\sigma_0}\right), \tag{2}$$

see Eq. 30 in Heimisson and Segall (2018) for detailed conditions for the validity of the approximation. Here $S(t) = \tau(t) - \mu\sigma(t)$ is the (modified) Coulomb stressing history, where $\mu = \tau_0/\sigma_0 - \alpha$. τ_0 and σ_0 are the initial background shear and effective normal stress respectively, α is the Linker-Dieterich constant (Linker & Dieterich, 1992).

The presence of the integral in Eq. 1 and the fact that $K(t) > 0$ causes perturbations introduced at $t = 0$ to decay. The (very) short time limit of Eq. 1, or alternatively the instantaneous response is simply:

$$R = rK(t) \approx r\exp\left(\frac{S(t)}{A\sigma_0}\right) \tag{3}$$

Dieterich (2007) argued that the instantaneous response (Eq. 3) is appropriate for periodic loading when the period T is small compared to a characteristic time, which describes when the seismicity rate starts decaying. We shall here investigate the validity of that arguement by Dieterich (2007), which has often been applied to tidal triggering of seismicity and tremor (e.g. Dieterich, 2007; Thomas et al., 2012; Delorey et al., 2017; Scholz et al., 2019).

We write the stressing history as the sum of steady stressing rate ($\dot{\tau}_0 t$) and time-dependent stress perturbation $S_T(t)$ and get

$$K(t) = \exp\left(\frac{S(t)}{A\sigma_0}\right) = \exp\left(\frac{S_T(t)}{A\sigma_0} + \frac{t}{t_a}\right) = \eta(t)\exp\left(\frac{t}{t_a}\right), \tag{4}$$

where $t_a = A\sigma_0/\dot{\tau}_0$. We assume $\eta(t)$ is an function with the following property

$$\eta(t) = M + \epsilon(t), \text{ where } M = \lim_{T\to\infty} \frac{1}{T}\int_0^T \eta(t)dt \text{ with } |M| < \infty, \tag{5}$$

it follows that

$$\lim_{T\to\infty} \frac{1}{T}\int_0^T \eta(t)dt = \lim_{T\to\infty} \frac{1}{T}\int_0^T Mdt + \frac{1}{T}\int_0^T \epsilon(t)dt = M + \lim_{T\to\infty} \frac{1}{T}\int_0^T \epsilon(t)dt. \tag{6}$$

In other words, M is the average of $\eta(t)$ and $|M| < \infty$, thus the average of $\epsilon(t)$ is zero, that is

$$\lim_{T\to\infty} \frac{1}{T}\int_0^T \epsilon(t)dt = 0. \tag{7}$$

For example, any periodic bounded function $\eta(t) = \eta(t{+}T)$, satisfies these conditions. In which case the physical interpretation of $\eta(t)$ is $\log(\eta(t)) = S_p(t)/A\sigma_0$ where $S_p(t) = S_p(t{+}T)$ is a periodic stress perturbation. There is no requirement that $S_p(t)$ be a harmonic pertubation, such as previously explored (Ader et al., 2014; Dieterich, 2007). If $\eta(t)$ is periodic then Eq. 4 describes a combination of steady stressing rate ($t_a = A\sigma_0/\dot{\tau}_0$) and a sum of periodic stress perturbations that represent the tidal loading. Tidal loading, and other oscillatory stresses, has multiple components and their periods do not exactly differ by a integer the resulting stressing history, which we shall call $S_T(t)$, is not periodic. However, we can still write $\eta(t) = \exp(S_T(t)/A\sigma_0) = M + \epsilon(t)$. Further, we could imagine that $\epsilon(t)$ contains a stochastic component. We shall now derive the long term behavior of a population of seismic sources that is persistently subject to a stressing history that can be written in the form of Eq. 4.

At intermediate times we may simplify Eq. 1

$$\frac{R(t)}{r} = \frac{K(t)}{\frac{1}{t_a}\int_0^t K(t')dt'}, \tag{8}$$

or using the form in Eq. 4

$$\frac{R(t)}{r} = \frac{\eta(t)\exp\left(\frac{t}{t_a}\right)}{\frac{1}{t_a}\int_0^t \eta(t)\exp\left(\frac{t}{t_a}\right)dt'}. \tag{9}$$

Substitution with 5 yields

$$\int_0^t \eta(t) \exp\left(\frac{t}{t_a}\right) dt' = t_a M \exp\left(\frac{t}{t_a}\right) + \int_0^t \epsilon(t') \exp\left(\frac{t'}{t_a}\right) dt' \tag{10}$$

and we get:

$$\frac{R(t)}{r} = \frac{\eta(t)}{M + \frac{1}{t_a}\int_0^t \epsilon(t') \exp\left(\frac{-(t-t')}{t_a}\right) dt'}. \tag{11}$$

We recognize that $\int_0^t \epsilon(t') \exp\left(\frac{-(t-t')}{t_a}\right) dt'$ is simply a convolution. The function $\exp(-(t-t')/t_a)$, imposes a memory effect and essentially eliminates any contribution in fluctuations in $\epsilon(t)$ in a time window of that lies significantly outside times $t - t_a$ to t. Thus if $\epsilon(t)$ averages to 0 on a timescales that is significantly shorter that t_a the integral can generally be ignored. For example, this condition is satisfied if the oscillatory stresses, and possible random stresses, average to approximately zero on a time-scale smaller than t_a. More precisely, the integral can be ignored if the following condition applies

$$\left| \frac{\frac{1}{t_a}\int_0^t \epsilon(t') \exp\left(\frac{-(t-t')}{t_a}\right) dt'}{M} \right| \ll 1, \text{ for all } t, \tag{12}$$

then equation 11 reduces to

$$\frac{R(t)}{r} = \frac{\eta(t)}{M} = \frac{\exp\left(\frac{S_T(t)}{A\sigma_0}\right)}{M}. \tag{13}$$

We have denoted the oscillatory contribution of the stresses as $S_T(t)$ and M is the average

$$M = \lim_{T\to\infty} \frac{1}{T} \int_0^T \exp\left(\frac{S_T(t)}{A\sigma_0}\right) dt. \tag{14}$$

Equation 13 generalizes the special cases for a harmonic perturbation that were explored by Ader et al. (2014). We note that oscillatory stress perturbations will take a 0 value at some time, in other words, at time t_0, $S_T(t_0) = 0$. The rate is

$$R_0 = \frac{r}{M},$$

Thus rate R is equal to the background average rate r is only when the there are no oscillatory stresses (that is $R_0 = r$ if $M = 1$), thus the validity of the theory proposed by Dieterich (2007) is limited to the case when the stress perturbation is very small compared to $A\sigma_0$ ($S_T(t)/A\sigma_0 \ll 1$). Since R_0 may be an observable it can be useful to rewrite Eq. 13

$$R(t) = R_0 \exp\left(\frac{S_T(t)}{A\sigma_0}\right). \tag{15}$$

Validity of equations 13/15

The validity of equations 13 and 15 rests on the the validity of Eq. 12. Two different expansions of the relevant term are possible through repeated integration by parts

$$\frac{1}{t_a}\exp\left(-\frac{t}{t_a}\right)\int \epsilon(t')\exp\left(\frac{t'}{t_a}\right)dt' = \frac{\epsilon^{-1}(t)}{t_a} - \frac{\epsilon^{-2}(t)}{t_a^2} + \frac{\epsilon^{-3}(t)}{t_a^3} + \ldots \tag{16}$$

$$\frac{1}{t_a}\exp\left(-\frac{t}{t_a}\right)\int \epsilon(t')\exp\left(\frac{t'}{t_a}\right)dt' = \epsilon - t_a\epsilon^{1}(t) + t_a\epsilon^{2}(t) - t_a^3\epsilon^{-3}(t) + \ldots \tag{17}$$

where ϵ^n is the n-th derivative of ϵ and ϵ^{-n} is the n-th indefinite integral (or anti-derivative) of ϵ. If the largest period, T_{max} in the Fourier decomposition of ϵ with a non-zero coefficient satisfies $T_{max} < t_a$ then the n-th term in Eq. 16 will be a correction of order $O(T_{max}^n/t_a^n)$, and convergence is expected. For long period changes $T_{min} > t_a$, equation 17 provides an expansion where we have $O(t_a^n/T_{min}^n)$ correction for the n-th term.

In the short period limit, $T_{max} < t_a$, we find a first order correction to Eq. 13:

$$\frac{R(t)}{r} = \frac{\exp\left(\frac{S_T(t)}{A\sigma_0}\right)}{M + \frac{\epsilon^{-1}(t)}{t_a}}, \tag{18}$$

where in practice we compute $\epsilon^{-1}(t)$ using the following equation unless the indefinite integral is known analytically.

$$\epsilon^{-1}(t) = \int_{-t_0}^{t} \exp\left(\frac{S_T(t)}{A\sigma_0}\right)dt - Mt,$$

where $t_0 > 0$ is chosen sufficiently large to erase the influence of the initial stress value in the integral. In the long period limit, , $T_{min} > t_a$, we get,

$$\frac{R(t)}{r} = \frac{\exp\left(\frac{S_T(t)}{A\sigma_0}\right)}{\exp\left(\frac{S_T(t)}{A\sigma_0}\right) - t_a\exp\left(\frac{S_T(t)}{A\sigma_0}\right)\frac{\dot{S}_T(t)}{A\sigma_0}} = \frac{1}{1 - t_a\frac{\dot{S}_T(t)}{A\sigma_0}}. \tag{19}$$

Equation 19 may be useful when investigating long term behavior such as seasonal changes if t_a is shorter than 1 year as is probably the case in active tectonic settings (e.g. Bettinelli et al., 2008). Notably, equation 19 depends on the stressing rate, not directly the stress. Implying that, in this particular limit, the seismicity rate is out of phase with the stress variations. Furthermore, we see that equation 13 is not valid in this limit since it predicts that the seismicity rate is proportional to the stress change, not the stressing rate.

3 Examples of applications and comparison with theory

3.1 Application to solid-earth tides

To test equation 13 against the full solution (equation 1) we generate a time series of Coulomb stress change using the *Solid* software (Milbert, 2018). The entire time-series is shown in Figure 1a, but we will restrict our attention to the observations window shown in Figure 1b. Most of the time series in Figure 1a is used to erase the initial response or initial conditions in equation 1 and compute M. In the following we referred to this procedure simply as erasing the initial response. We choose $t_a = 0.5$ years. We vary $A\sigma_0$ as described in Figure 2 choosing rather low values that yield a particularly large response. We find that even for large fluctuations in R/r, equation 13 is in good agreement with the full solution (Figure 2c).

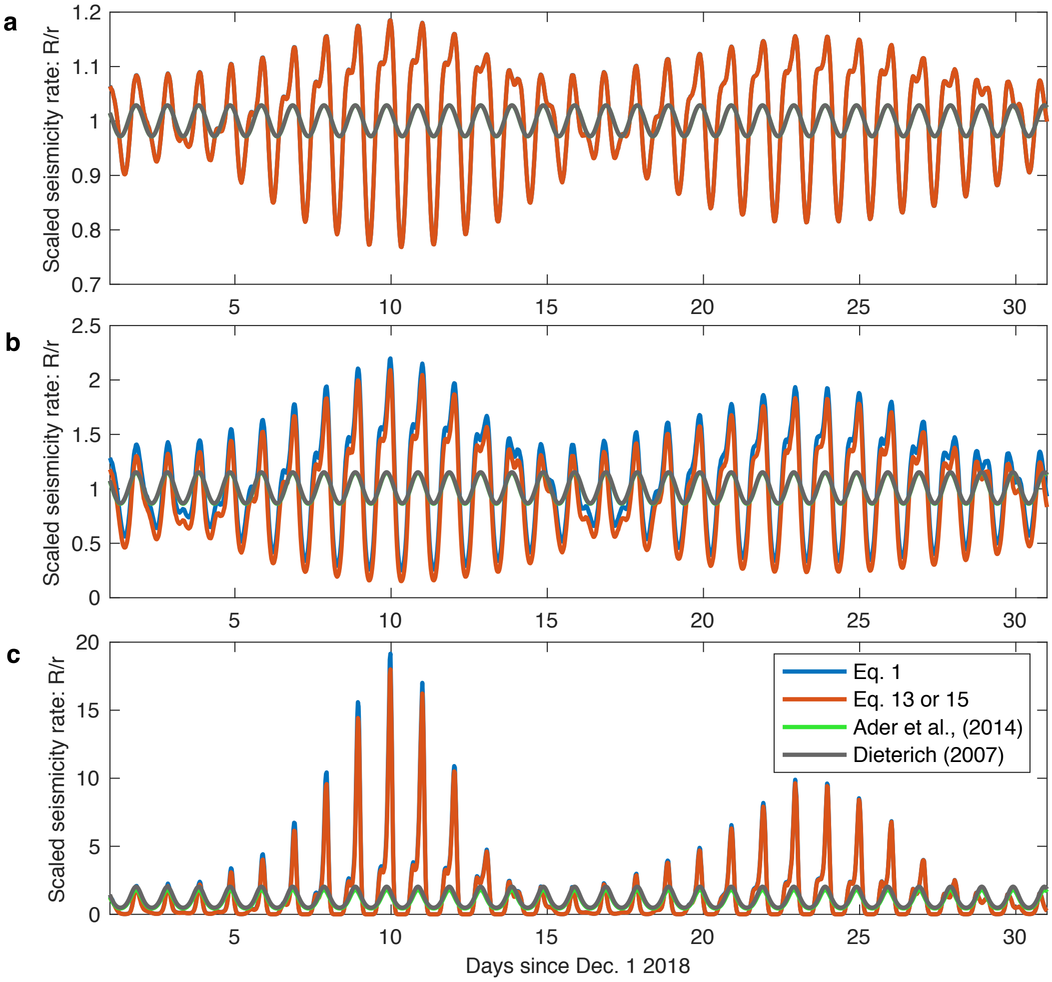

Figure 2. Comparison of various approximations and the full solution in equation 1 after the initial response has been faded out. Scaled seismicity rate (R/r) for (a) $A\sigma_0 = 5 \cdot 10^{-3}$ MPa, (b) $A\sigma_0 = 2 \cdot 10^{-3}$ MPa, (c) $A\sigma_0 = 1 \cdot 10^{-4}$ MPa. In all cases equation 13 provides an excellent approximation. A single harmonic perturbation does not capture the details of the curve shape or amplitude.

Corresponding theory for a single harmonic stress perturbation has been previously reported and is not repeated here for the sake of brevity. We computed the dominant frequency of the signal in Figure 1a, by computing a power spectral density. Then find the best fitting amplitude and phase by minimizing an L_2 norm that quantifies the residual between the time-series shown in Figure 1a and the single harmonic function. The resulting stress perturbations are then used to compute the seismicity rate using both the expressions from Dieterich (2007) and Ader et al. (2014) in Figure 2. Using the dominant frequency of the earth-tide signal generally predicts when the seismicity rate is higher or lower than average. However, the shape and amplitude of the theoretical seismicity rate time-series cannot be matched with a single harmonic function.

3.2 Marsquakes: Reevaluating Manga et al. (2019)

Recently, Manga et al. (2019) argued that Mars might have a clearer relationship between tides and seismicity rate, which could result in variation as large as two orders of magnitude in scaled seismicity rate R/r, also known as relative seismicity rate (see Figure 3 bottom-left panel in Manga et al. (2019)). As we show, their predicted signal was apparently produced based on the initial instantaneous response (Figure 3a) and thus incorrect. As discussed in the previous section, care needs to be taken to erase the initial response when applying equation 1 by simulating a period of time before the observation window that is much larger than t_a and is sufficiently long to estimate M accurately. If this is not done, the tidal response may be significantly over-estimated, indeed by a factor of $1/M$.

We use equation 1 without erasing the initial response and find a good agreement with their results (Figure 3a), in spite of some simplifying assumptions we make that are detailed in the next paragraph. Extrapolation of their results suggest that the changes in seismicity rate should be much smaller than they estimated (Figure 3b) .

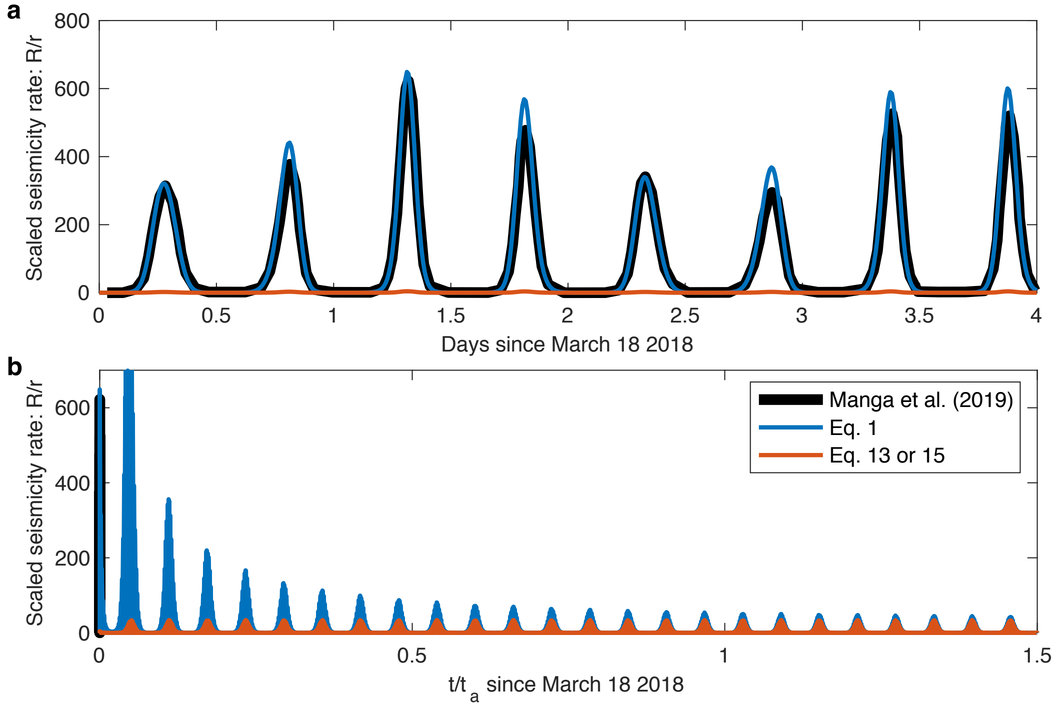

Figure 3. Reevaluation of Manga et al. (2019), reveals that they likely overestimated the their maximum response at least a factor of 10. (a) using an approximate stressing history we observe that equation 1 is in good agreement with the results reported in Figure 3 bottom-left panel in Manga et al. (2019), whereas equation 13 suggests that the amplitude should be approximately 100 times less. (b) Simulating a time-scale $t \sim t_a$, where $t_a \approx 71.5$ earth years, shows that equation 1 and 13 appear to converge once the initial response gets erased.

To replicate the results of Manga et al. (2019), we simply approximate the Coulomb stress perturbations they reported for strike $= 0°$ (Figure 2 in Manga et al. (2019)) by a sum of three harmonic functions fitted to a digitized version of their figure. This provides an excellent fit to the reported Coulomb stress calculations during the four days window they show. However, the long term extrapolation shown in Figure 3b shows that the seismicity rate decays over a time-scale of $t \sim t_a$, before reaching the true expected rate due to tidal loading. The transient high seismicity rate would not be observable and only the long term steady response should be considered observable. We appreciate and respect the original and forward-looking work of Manga et al. (2019), but claim that their maximum estimated seismicity response to tidal forcing is likely overestimated by at least one order of magnitude.

4 Discussion

Equations 13 or 15 offer an estimate of the seismicity rate produced by a population of seismic sources due to a stressing history, which is produced by a constant stressing rate and oscillating stress sources. These equations are perfectly equivalent and simple to use, given that the stressing history is known, there is only one free parameter that may need to be fitted: $A\sigma_0$. In case of observations of a seismicity response to a known stressing history, they might thus be used to assess the validity of the theory for seismicity rate based on rate-and-state friction (Dieterich, 1994; Heimisson & Segall, 2018) and place constraints on the friction law. Further, establishing $A\sigma_0$ by using tides or seasonal stress variations has implications for physics-based forecasts of aftershocks, where this parameter also needs to be estimated (e.g. Hainzl et al., 2010). Thus tides could be used in advance to constrain the value as a function of geographic location. Then those values could be used for aftershock forecasts once an earthquake occurs.

Equation 15 maybe more useful in data applications than 13 since it does not require knowledge of the long-term stressing history and R_0 can be simply estimated from the observed rate as the calculated Coulomb stresses passes through $S_T = 0$. Remarkably, Scholz et al. (2019) used Eq. 15 in their study in good agreement with data. They, however, referred to R as "the instantaneous seismicity rate". As we have shown here R in equation 3 represents the instantaneous seismicity rate, but equation 15 is the approximate seismicity rate in the presence of long term response tidal loading or other oscillatory stresses. $R_0 \neq r$, unless $|S_T(t)|/A\sigma_0 \ll 1$ for all t, in which case $R_0 \approx r$.

The approximation made in equation 13 or 15 is not valid in the limit of a very long period stress variations that are larger than t_a as described by equation 19. In this case, we expect the seismicity rate to be proportional to the stressing rate, but not the stress. Beeler and Lockner (2003) conducted experiments on a saw-cut sample in a triaxial loading frame. They imposed oscillatory stresses on a constant stressing rate and found that for short periods compared to the nucleation time, changes in event probability was in phase with the stress. However, for long periods the events probability was in phase with the stressing rate. Their finding is in agreement with our theoretical results. Johnson et al. (2017) investigated the relationship between seismicity rate and seasonal variations in shear stress and stress rate in California. Depending on fault orientation, they identified a weak correlation of seismicity rate with either shear stressing rate or stress. This finding would suggest that on average t_a changes with fault orientation. That is reasonable since background stressing rates must vary with fault orientation. We emphasize that when investigating seasonal changes in seismicity rate, which may be on a similar time-scale as t_a, one has to be careful in picking the appropriate approximation (either 13 or 19). We strongly suggest that equation 1 should be used for reference after having erased the initial response. Further, we recall that our analysis assumes that a single degree of freedom spring-and-slider system can approximate the response of a fault to a stress perturbation. Significant differences have been observed if finite fault effects need to be taken into account (e.g. Kaneko & Lapusta, 2008; Ampuero & Rubin, 2008; Rubin & Ampuero, 2005). Simulations indicate that this happens if the typical period of the stress perturbation is of the order of $2\pi t_a$ (Ader et al., 2014). In that case, the analytical solutions described in this study would not apply.

Using a single harmonic function to represent the oscillating stressing history may be desirable due to the simplicity of the problem and the fact that spectral analysis, such as the Schuster spectra, can be used to extract the dominant period of the seismicity rate (Ader et al., 2014). However, this may lead to a bias in the estimate of $A\sigma_0$ if the stressing history has multiple components that can add up coherently. Let us assume that the stressing history is composed of N harmonic components:

$$S_T(t) = \sum_{i=1}^{N} c_i \sin\left(\frac{2\pi t}{T_i} + \phi_i,\right) \tag{20}$$

where the amplitudes are sorted: $c_1 < c_2 < \ldots < c_N$ and thus T_1 is the dominant period. Using equation 15 and only the dominant harmonic component of the $S_T(t)$ then one finds:

$$\log\left(\frac{\max(R)}{R_0}\right) = \frac{c_1}{(A\sigma_0)_{SH}}, \tag{21}$$

where $(A\sigma_0)_{SH}$ represent the estimate of $A\sigma_0$ under the assumption of a single harmonic, and $\max(R)$ is the maximum observed seismicity rate. However, for multiple harmonics we find:

$$\log\left(\frac{\max(R)}{R_0}\right) = \max\left(\frac{\sum_{i=1}^{N} c_i \sin\left(\frac{2\pi t}{T_i} + \phi_i,\right)}{(A\sigma_0)_{MH}}\right) \leq \frac{\sum_{i=1}^{N} c_i}{(A\sigma_0)_{MH}}, \tag{22}$$

where $(A\sigma_0)_{MH}$ represent the estimate of $A\sigma_0$ under the assumption of multiple harmonics. Thus we conclude that the ratio of the two estimates is bounded in the following manner

$$\frac{(A\sigma_0)_{MH}}{(A\sigma_0)_{SH}} \leq \frac{\sum_{i=1}^{N} c_i}{c_1}. \tag{23}$$

We, therefore, expect that $A\sigma_0$ is typically underestimated if a single harmonic stress source is assumed. This conclusion is consistent with Figure 2, which shows that that the amplitude is not well match by a single harmonic, but reducing $A\sigma_0$ could provide better agreement, but the inferred value of $A\sigma_0$ would be systematically underestimated.

5 Conclusions

We have derived a simple approximate equation for the relationship between seismicity and oscillatory stresses, for example, due to tidal or seasonal loading, based on rate-and-state friction. This relationship may be used in theoretical or observations studies (equation 13 or 15). In applications to observations, only one free parameter ($A\sigma_0$) needs to be determined. We compare our approximations to using the dominant harmonic mode of the stresses and to the full solution (1) where the initial response has been carefully erased. We conclude that in most cases, our approximation is in excellent agreement with the full solution and is much more accurate than using a single harmonic stress perturbation as an approximation. We find that Manga et al. (2019) very likely overestimated the changes in seismicity rate due to tides on Mars. We have here provided a simple equation 13 that may be used to reevaluate this effect or, more generally, the seismicity response expected from stress variations on Earth and solid-surface bodies, provided that fault finite-size effects can be neglected.

Acknowledgments

This is a theoretical paper and contains no data. This research was partly supported by NSF award EAR-1821853.

References

Ader, T. J., Lapusta, N., Avouac, J.-P., & Ampuero, J.-P. (2014, 05). Response of rate-and-state seismogenic faults to harmonic shear-stress perturbations. *Geo-*

physical Journal International, *198*(1), 385-413. doi: 10.1093/gji/ggu144

Amos, C. B., Audet, P., Hammond, W. C., Bürgmann, R., Johanson, I. A., & Blewitt, G. (2014). Uplift and seismicity driven by groundwater depletion in central california. *Nature*, *509*(7501), 483–486. doi: 10.1038/nature13275

Ampuero, J.-P., & Rubin, A. M. (2008). Earthquake nucleation on rate and state faults – aging and slip laws. *Journal of Geophysical Research: Solid Earth*, *113*(B1). doi: 10.1029/2007JB005082

Beeler, N. M., & Lockner, D. A. (2003). Why earthquakes correlate weakly with the solid earth tides: Effects of periodic stress on the rate and probability of earthquake occurrence. *Journal of Geophysical Research: Solid Earth*, *108*(B8). doi: 10.1029/2001JB001518

Bettinelli, P., Avouac, J.-P., Flouzat, M., Bollinger, L., Ramillien, G., Rajaure, S., & Sapkota, S. (2008). Seasonal variations of seismicity and geodetic strain in the himalaya induced by surface hydrology. *Earth and Planetary Science Letters*, *266*(3), 332–344. doi: 10.1016/j.epsl.2007.11.021

Chanard, K., Nicolas, A., Hatano, T., Petrelis, F., Latour, S., Vinciguerra, S., & Schubnel, A. (2019). Sensitivity of acoustic emission triggering to small pore pressure cycling perturbations during brittle creep. *Geophysical Research Letters*, *46*(13), 7414-7423. doi: 10.1029/2019GL082093

Cochran, E. S., Vidale, J. E., & Tanaka, S. (2004). Earth tides can trigger shallow thrust fault earthquakes. *Science*, *306*(5699), 1164–1166. doi: 10.1126/science.1103961

Delorey, A. A., van der Elst, N. J., & Johnson, P. A. (2017). Tidal triggering of earthquakes suggests poroelastic behavior on the san andreas fault. *Earth and Planetary Science Letters*, *460*, 164 - 170. doi: https://doi.org/10.1016/j.epsl.2016.12.014

Dieterich, J. (1994). A constitutive law for rate of earthquake production and its application to earthquake clustering. *J. Geophys. Res. Solid Earth*, *99*(B2), 2601–2618. doi: 10.1029/93JB02581

Dieterich, J. (2007). 4.04 - applications of rate- and state-dependent friction to models of fault-slip and earthquake occurrence. In G. Schubert (Ed.), *Treatise on geophysics (second edition)* (Second Edition ed., p. 93 - 110). Oxford: Elsevier. Retrieved from `http://www.sciencedirect.com/science/article/`

pii/B9780444538024000750 doi: https://doi.org/10.1016/B978-0-444-53802-4.00075-0

Duennebier, F., & Sutton, G. H. (1974). Thermal moonquakes. *Journal of Geophysical Research (1896-1977)*, *79*(29), 4351-4363. doi: 10.1029/JB079i029p04351

Hainzl, S., Brietzke, G. B., & Zoller, G. (2010). Quantitative earthquake forecasts resulting from static stress triggering. *Journal of Geophysical Research: Solid Earth*, *115*(B11). doi: 10.1029/2010JB007473

Hawthorne, J. C., & Rubin, A. M. (2010). Tidal modulation of slow slip in cascadia. *Journal of Geophysical Research: Solid Earth*, *115*(B9). doi: 10.1029/2010JB007502

Heimisson, E. R. (2019). Constitutive law for earthquake production based on rate-and-state friction: Theory and application of interacting sources. *Journal of Geophysical Research: Solid Earth*, *124*(2), 1802-1821. doi: 10.1029/2018JB016823

Heimisson, E. R., & Segall, P. (2018). Constitutive law for earthquake production based on rate-and-state friction: Dieterich 1994 revisited. *Journal of Geophysical Research: Solid Earth*, *123*(5), 4141–4156. doi: 10.1029/2018JB015656

Houston, H. (2015). Low friction and fault weakening revealed by rising sensitivity of tremor to tidal stress. *Nature Geoscience*, *8*(5), 409–415. doi: 10.1038/ngeo2419

Johnson, C. W., Fu, Y., & Bürgmann, R. (2017). Seasonal water storage, stress modulation, and california seismicity. *Science*, *356*(6343), 1161–1164. doi: 10.1126/science.aak9547

Johnson, C. W., Fu, Y., & Bürgmann, R. (2020). Hydrospheric modulation of stress and seismicity on shallow faults in southern alaska. *Earth and Planetary Science Letters*, *530*, 115904. doi: 10.1016/j.epsl.2019.115904

Kaneko, Y., & Lapusta, N. (2008). Variability of earthquake nucleation in continuum models of rate-and-state faults and implications for aftershock rates. *Journal of Geophysical Research: Solid Earth*, *113*(B12). doi: 10.1029/2007JB005154

Linker, M. F., & Dieterich, J. H. (1992). Effects of variable normal stress on rock friction: Observations and constitutive equations. *J. Geophys. Res. Solid Earth*, *97*(B4), 4923–4940. doi: 10.1029/92JB00017

Lognonne, P. (2005). Planetary seismology. *Annual Review of Earth and Planetary Sciences*, *33*(1), 571–604. doi: 10.1146/annurev.earth.33.092203.122604

Lu, Z., Yi, H., & Wen, L. (2018). Loading-induced earth's stress change over time. *Journal of Geophysical Research: Solid Earth*, *123*(5), 4285-4306. doi: 10.1029/2017JB015243

Luo, Y., & Liu, Z. (2019). Slow-slip recurrent pattern changes: Perturbation responding and possible scenarios of precursor toward a megathrust earthquake. *Geochemistry, Geophysics, Geosystems*, *20*(2), 852-871. doi: 10.1029/2018GC008021

Manga, M., Zhai, G., & Wang, C.-Y. (2019). Squeezing marsquakes out of groundwater. *Geophysical Research Letters*, *46*(12), 6333-6340. Retrieved from `https://agupubs.onlinelibrary.wiley.com/doi/abs/10.1029/2019GL082892` doi: 10.1029/2019GL082892

Milbert, D. (2018). *Solid.* `https://geodesyworld.github.io/SOFTS/solid.htm`. (version update used: 2018-Jun-07)

Ross, Z. E., Trugman, D. T., Hauksson, E., & Shearer, P. M. (2019). Searching for hidden earthquakes in southern california. *Science*, *364*(6442), 767–771. Retrieved from `https://science.sciencemag.org/content/364/6442/767` doi: 10.1126/science.aaw6888

Rubin, A. M., & Ampuero, J.-P. (2005). Earthquake nucleation on (aging) rate and state faults. *Journal of Geophysical Research: Solid Earth*, *110*(B11). doi: 10.1029/2005JB003686

Rubinstein, J. L., La Rocca, M., Vidale, J. E., Creager, K. C., & Wech, A. G. (2008). Tidal modulation of nonvolcanic tremor. *Science*, *319*(5860), 186–189. doi: 10.1126/science.1150558

Scholz, C. H., Tan, Y. J., & Albino, F. (2019). The mechanism of tidal triggering of earthquakes at mid-ocean ridges. *Nature communications*, *10*(1), 2526. doi: 10.1038/s41467-019-10605-2

Tanaka, S. (2012). Tidal triggering of earthquakes prior to the 2011 tohoku-oki earthquake (mw 9.1). *Geophysical Research Letters*, *39*(7). doi: 10.1029/2012GL051179

Tanaka, S., Ohtake, M., & Sato, H. (2002). Evidence for tidal triggering of earthquakes as revealed from statistical analysis of global data. *Journal of Geophys-*

ical Research: Solid Earth, *107*(B10). doi: 10.1029/2001JB001577

Thomas, A. M., Bürgmann, R., Shelly, D. R., Beeler, N. M., & Rudolph, M. L. (2012). Tidal triggering of low frequency earthquakes near parkfield, california: Implications for fault mechanics within the brittle-ductile transition. *Journal of Geophysical Research: Solid Earth*, *117*(B5). doi: 10.1029/2011JB009036

Thomas, A. M., Nadeau, R. M., & Bürgmann, R. (2009). Tremor-tide correlations and near-lithostatic pore pressure on the deep san andreas fault. *Nature*, *462*(7276), 1048–1051. doi: 10.1038/nature08654

Tolstoy, M., Vernon, F. L., Orcutt, J. A., & Wyatt, F. K. (2002). Breathing of the seafloor: Tidal correlations of seismicity at Axial volcano. *Geology*, *30*(6), 503-506. doi: 10.1130/0091-7613(2002)030<0503:BOTSTC>2.0.CO;2

Ueda, T., & Kato, A. (2019). Seasonal variations in crustal seismicity in san-in district, southwest japan. *Geophysical Research Letters*, *46*(6), 3172–3179. doi: 10.1029/2018GL081789

Yabe, S., Tanaka, Y., Houston, H., & Ide, S. (2015). Tidal sensitivity of tectonic tremors in nankai and cascadia subduction zones. *Journal of Geophysical Research: Solid Earth*, *120*(11), 7587-7605. doi: 10.1002/2015JB012250